

# Theoretical Examination on Significantly Low Off-State Current of a Transistor using Crystalline In-Ga-Zn Oxide

Masakazu Murakami, Kiyoshi Kato, Ko Inada, Takanori Matsuzaki, Yasuyuki Takahashi and Shunpei Yamazaki

Semiconductor Energy Laboratory Co., Ltd., 398 Hase, Atsugi, Kanagawa, 243-0036, Japan

Phone: +81-46-248-1131 Fax : +81-46-270-3751 E-mail: kkato@sel.co.jp

## 1. Introduction

Crystalline oxide semiconductors have attracted attention as materials for next-generation thin film transistors. In particular, crystal structures of  $\text{InGaO}_3(\text{ZnO})_m$  were found in 1985 by Kimizuka *et al* [1]. Noticeable findings of our extensive studies on  $\text{InGaZnO}_4$  (IGZO) thin films [2] are that our IGZO has a c-axis aligned crystal (CAAC) structure [3] and that an IGZO FET having a CAAC structure has a significantly low off-state current on the order of  $\text{yA}$  per  $\mu\text{m}$  of channel width ("y" (yocto) denotes  $10^{-24}$ ) [4,5].

Clarifying mechanisms underlying the low off-state current contributes to development of nonvolatile circuit technologies [6] and low power technologies [7] with IGZO FETs. This report presents a theoretical examination of the origin of significantly low off-state current, through a comparison with a Si FET. In particular, drain-to-channel tunneling of holes will be discussed as a mechanism governing the off-state current of IGZO FETs.

## 2. Experimental Results

Fig. 1 shows  $V_G$ - $I_D$  characteristics of a fabricated CAAC-IGZO FET which has an overlap between the gate and the source/drain electrodes. For detection of the off-state current, 20000 FETs each having a channel length of  $3 \mu\text{m}$  and a channel width of  $50 \mu\text{m}$  are connected in parallel to have a total channel width of  $1 \text{ m}$ . It is confirmed that the off-state current is below the measurement limit ( $1 \times 10^{-13} \text{ A}$ ). The off-state current is even lower, and about  $50 \text{ yA}$  per  $\mu\text{m}$  of channel width is reported [4,5].

## 3. Theoretical Examination

Fig. 2 shows a band diagram of the IGZO FET in the off state with a positive  $V_D$  and a negative  $V_G$ . The band diagram is based on physical properties shown in Table I. Note that the source/drain electrodes are directly connected to the IGZO channel region.

Three possible major mechanisms for off-state current are: 1) injection of thermally excited electrons from the source into the channel, 2) injection of thermally excited holes from the drain into the channel, and 3) tunneling of holes from the drain to the channel.

The amount of leakage current due to 1) thermally excited electrons is proportional to  $\exp(-\Delta E_{\text{ele}}/k_B T)$ . Here,  $\Delta E_{\text{ele}} (= E_C - E_F)$  denotes a potential barrier for electrons and becomes substantially equal to the band gap by lowering the gate voltage. In such a case, the ratio between exponential factors of the IGZO FET and the Si FET is  $\exp(-(E_g(\text{IGZO}) - E_g(\text{Si}))/k_B T) \sim 10^{-35}$  which is significantly small, and this means the leakage current due to thermally excited electrons is negligible.

The amount of leakage current due to 2) thermally excited holes is proportional to  $\exp(-\Delta E_{\text{hole}}/k_B T)$ . Here,  $\Delta E_{\text{hole}}$  of the IGZO FET denotes a potential barrier at the drain edge, and  $\Delta E_{\text{hole}}$  is found to be  $2.8 \text{ eV}$  from Table I, while  $\Delta E_{\text{hole}}$  of the Si FET is considered roughly similar to  $E_g(\text{Si})$ .

The ratio between these exponential factors is  $\exp(-(2.8 \text{ eV} - E_g(\text{Si}))/k_B T) \sim 10^{-27}$  which is significantly small, and this demonstrates that the leakage current due to thermally excited holes is also negligible.

Now, 3) drain-to-channel tunneling of holes is discussed. A simplified model is considered, where a particle passes through a one-dimensional triangular potential barrier with height  $V_0$  and width  $a$ , and  $m$  and  $m^*$  are the effective masses of the particle at  $x < 0$  and at  $x \geq 0$ , respectively. The tunneling current density  $J$  obtained when a particle impinges on the barrier from a region with  $x < 0$  and tunnels through a region with  $0 \leq x \leq a$  to a region with  $x > a$  can be given by a Fowler-Nordheim-type equation at  $0 \text{ K}$ :

$$J = \frac{q^3 F^2}{8h\pi V_0} \sqrt{\frac{m}{m^*}} \exp\left(-\frac{8\pi\sqrt{2m^*}}{3qhF} V_0^{3/2}\right), \quad (1)$$

where  $V_0$  is barrier height,  $F = V_0/a$  is electric field intensity,  $h$  is Planck's constant, and  $q$  is elementary charge. In this case, the particle corresponds to a hole, the region with  $x < 0$ , a drain, and the region with  $x \geq 0$ , a channel. This means  $m^*$  in the exponential part corresponds to the effective mass of a hole in IGZO. The tunneling current density  $J$  is calculated as below using  $m^*$  estimated by first-principles calculations and  $V_0$  and  $a$  estimated by device simulations.

### Calculation of effective masses of holes

Fig. 3 shows a crystal structure of IGZO [8] used for the calculation. A perfect crystal is assumed. The total number of atoms in the unit cell is 84. The norm-conserving pseudopotential DFT employed in OpenMX [9] is used, and the PBE GGA is used for the exchange interaction potential of electrons. The cut-off energy of the local basis function is set at  $200 \text{ Ryd}$ , and the k-point sampling is conducted using a  $5 \times 5 \times 3$  mesh.

Fig. 4 is the calculated energy band diagram, which shows that the distribution of the valence band is significantly flat compared with that of the conduction band.

Table II shows the effective masses of holes and electrons in IGZO and Si. Holes in IGZO are heavy with effective masses of 10 or more, which strongly suppress the flow of tunneling current.

### Calculation of height and width of tunneling barrier

Fig. 5 is the band diagram near the drain edge obtained by device simulations using Sentaurus Device (Synopsys, Inc.) [10], where the channel length, the gate insulator thickness, the relative permittivity, the donor concentration,  $V_G$ , and  $V_D$  are  $3 \mu\text{m}$ ,  $30 \text{ nm}$ ,  $15$ ,  $10^{-10} \text{ cm}^{-3}$ ,  $3 \text{ V}$ , and  $5 \text{ V}$ , respectively. The diagram confirms that the triangular potential approximation is valid.

Table III shows parameters of the potential barrier in the IGZO FET and those in the Si FET obtained by similar calculations. The potential barrier in the IGZO FET is found to be about three times as large as that in the Si FET.

### Hole tunneling current density

From the above calculations, the hole tunneling current density is found as shown in Table IV. The hole tunneling current density in the IGZO FET is substantially zero as compared with that in the Si FET.

### 4. Conclusions

Significantly low drain-to-channel hole tunneling current in the IGZO FET has been proved by heavy holes with effective masses of 10 or more, and a large tunneling barrier with a height of 2.8 eV and a width of 25 nm. This result is supported by the experimental fact that the off-state in the IGZO FET is significantly low.

The results based on a perfect crystal require more practical future examinations. Nevertheless, we have successfully revealed that significantly low hole tunneling current is due to heavy holes in IGZO FETs, which strongly suggests that IGZO FETs have suitable features for non-volatile circuits and low power technologies.

### References

- [1] N. Kimizuka and T. Mohri, J. Solid State Chem. **60**, 382 (1985).
- [2] S. Yamazaki, presented at the Int. Workshop Private Sector – Academia Interactions (2011).
- [3] M. Takahashi *et al.*, Proc. AM-FPD'11 Digest, (2011) 271.
- [4] Y. Sekine *et al.*, ECS Trans. **37**, 77 (2011).
- [5] K. Kato *et al.*, Jpn. J. Appl. Phys. **51** (2012) 021201.
- [6] T. Matsuzaki *et al.*, in *IEEE IMW, 2011*, p.185.
- [7] S. Amano *et al.*, SID Int. Symp. Dig. Tech. Pap. **41**, 626 (2010).
- [8] M. Takahashi *et al.*, Proc. AM-FPD'08 Digest, (2008) 1637.
- [9] T. Ozaki and H. Kino, Phys. Rev. B **69**, 195113 (2004).
- [10] *Sentaurus Device User Guide* (Synopsys, Inc., 2010).

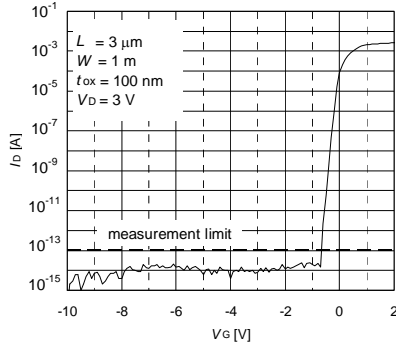


Fig. 1  $V_G$ - $I_D$  curve of the CAAC-IGZO FET.

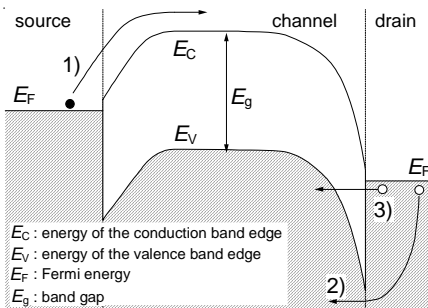


Fig. 2 Schematic band diagram of the IGZO FET in the off state.

Table I Physical properties

	measured value	measurement method
ion energetic of IGZO	7.8eV	UPS
band gap of IGZO	3.2eV	ellipsometer
work function of tungsten(W)	5.0eV	UPS

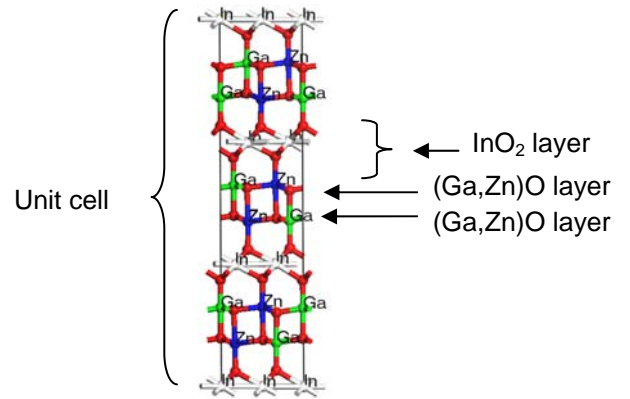


Fig. 3 Crystal structure of IGZO.

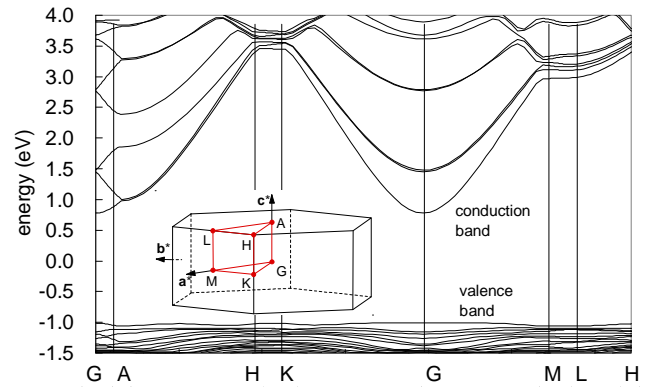


Fig. 4 Energy band diagram of crystalline IGZO.

Table II Effective masses of holes and electrons

material	hole effective mass $m_h^*/m_0$	electron effective mass $m_e^*/m_0$
IGZO	21(a*), 41(b*), 11(c*)	0.25(a*), 0.25(b*), 0.23(c*)
Si	0.49 (heavy) 0.16 (light)	0.98 (longitudinal) 0.19 (transverse)

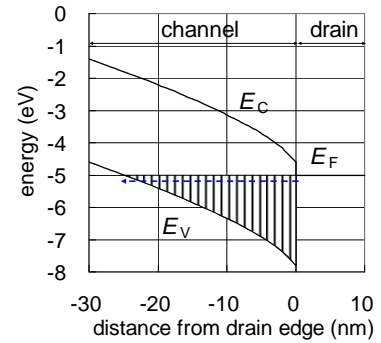


Fig. 5 Band diagram of the IGZO FET in the off state.

Table III Parameters for tunneling current density  $J$

parameter	IGZO FET	Si FET
$V_0$ (eV)	2.8	1.1
$a$ (nm)	25	7
$F=V_0/a$ (MV/m)	112	157

Table IV Hole tunneling current density

	IGZO FET	Si FET
tunneling current density $J$ (yA/ $\mu\text{m}^2$ )	$\sim \exp(-900)$	$1.8 \times 10^{14}$